A High Resolution Microprobe Study of EETA79001 Lithology C

C.M. Schrader[1], B.A. Cohen[2], J.J. Donovan[3], and E.P. Vicenzi[4]. [1]NASA Postdoctoral Program-MSFC (Christian.M.Schrader@nasa.gov),
[2]NASA-MSFC, [3]University of Oregon Department of Chemistry, [4]Smithsonian Institution, Museum Conservation Institute

Background

Antarctic meteorite EETA79001 has received substantial attention for possibly containing a component of Martian soil in its impact glass (Lithology C) [1]. The composition of Martian soil can illuminate near-surface processes such as impact gardening [2] and hydrothermal and volcanic activity [3,4]. Impact melts in meteorites represent our most direct samples of Martian regolith.

We present the initial findings from a high-resolution electron microprobe study of Lithology C from Martian meteorite EETA79001. As this study develops we aim to extract details of a potential soil composition and to examine Martian surface processes using elemental ratios and correlations.

Sample description

Thin section EETA79001,18 contains pools of non-crystalline impact melt glass up to several hundred microns across and mixed domains of dendritic crystals, mostly olivine, with interstitial glass. These quench textures are interpreted to have formed by incipient crystallization of the impact melt. This section also contains sub-rounded olivine and sparse S- and P-rich grains that may represent partially fused relict grains.

Analysis and approach

We conducted semi-quantitative EDS and quantitative WDS elemental mapping on the Cameca SX-100 electron microprobe at the CAMCOR facility in Eugene, Oregon. EDS datasets were generated for two areas of 1024 by 768 pixels at ~0.3 µm/pixel. WDS elemental datasets were generated with a focused beam (<1µm) operating at 12 keV and 50 nA. EDS data were processed using Thermo NSS software and WDS data were processed using the Probe for EPMA software package.

We are working to assess pre-impact compositions in the melt. Possible sources are: Lithology A (the host basalt), excess plagioclase from comminution of bedrock, and the Martian soil [1]. Martian soil contains excess Ni from olivine weathering [5,6] and salts and sulfates-species from hydrothermal fluids, volcanic aerosols, or evaporitic processes [3,4,7] .

For example, if excess sulfur is contributed by melted soil, S might be expected to correlate positively with other elements rich in soil but poor in Lithology A, such as Cl and Ni. Conversely, if S is correlated with elements like Fe, this may point to a host-rock source for the S, such as Lithology A sulfides.

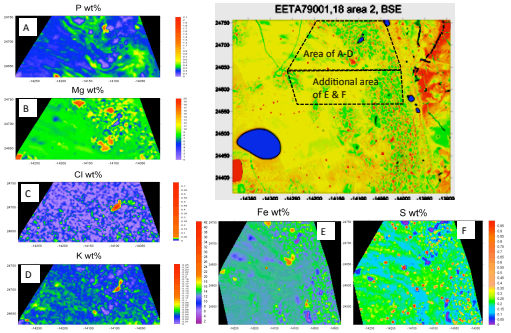

Figure 1. BSE image and WDS-derived element maps for section EETA79001A, area 2. Coordinates are in microns. Note that the scale for E and F differs from the other maps.

WDS results

Figure 1 shows element maps and a backscatter electron (BSE) images for one area of the thin section. Magnesium and Fe are concentrated in areas of crystallization. Chlorine is relatively low throughout except for one area that corresponds to high K values. Most of the highest S occurrences correspond to high Fe; apart from the highest concentrations, S shows complex gradients in the melt portions.

EDS results

Figure 2 contains EDS-derived element maps for a region dominated by olivine quench crystals in impact melt. The lower right hand corner is a pod of pure melt. There are larger olivine grains on which quench crystals are nucleating and several small grains of S- and P-bearing minerals.

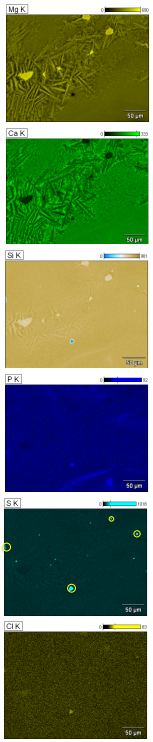

Figure 2. EDS element maps for area 5, based on Kα peaks. Circled grains in the S map have high Fe, while other grains do not.

Magnesium is concentrated in olivine. Calcium is concentrated around olivine crystals, where it is preferentially enriched by the removal of Mg, Fe, and Si from the melt. The Si map distinctly shows the two largest non-silicate grains – both of which have high relative concentrations of Fe (not shown), S, and Cl and moderately high concentrations of P. Phosphorous occurs in this Fe-S-P-Cl grain but it is present in almost equal proportions as streaks in the impact melt. These high-phosphorous melt zones are also slightly elevated in Ca and depleted in Si; one zone runs along the crystallization front and the other is in the center of the melt pool. Sulfur occurs with Fe in grains circled in Figure 2. This includes both the above-mentioned grains and other apparent Fe-sulfides or Fe-sulfates. Additionally, S is concentrated in a number of other small grains or regions without any other determined elements – these may be sulfides or sulfates with undetermined cations or S-rich portions of interstitial melt. Chlorine occurs in detectable amounts at a low background level and in the Fe-S-P-Cl grains.

Data analysis

We exported EDS data for the area shown in Figure 2 into spreadsheets for statistical analysis in Excel and StatistXL, including correlation and principal component analysis (PCA). Figure 3 contains a gray scale image of this region and of the subregion of pure melt for which data was extracted for a second experiment.

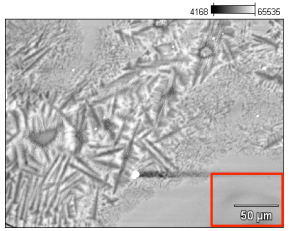

Figure 3. Gray-scale map for area 5, also shown in Figure 2. We performed statistical analyses on the entire region and for the corner of pure melt designated by the red square.

PCA results

We show components with eignenvalues ≥ 1.0. The total variance explained by these components if 53% and 46%, respectively. See Figure 3 for experimental regions.

Experiment 1: total area

Eigenvectors				
Variable	PC 1	PC 2	PC 3	PC 4
Si	0.415	-0.299	-0.236	-0.044
Al	0.438	0.044	0.312	0.011
Ti	0.072	0.174	-0.143	-0.212
Fe	-0.300	0.462	-0.115	0.018
Mg	-0.491	-0.403	0.022	-0.001
Ca	0.482	0.324	-0.116	-0.002
Na	0.024	-0.148	0.819	-0.050
K	0.082	0.063	0.076	0.686
P	0.041	0.217	0.303	-0.077
S	-0.221	0.550	0.168	0.007
Cl	-0.081	0.088	-0.047	0.452
Ni	-0.040	0.122	0.021	-0.518
Eigenval.	2.49	1.82	1.06	0.99
Cum.%	20.8	35.9	44.8	53.1

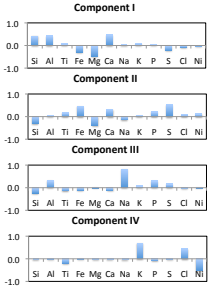

Experiment 2: melt corner

Eigenvectors				
Variable	PC 1	PC 2	PC 3	PC 4
Si	0.052	-0.713	-0.141	-0.169
Al	0.569	0.014	-0.004	-0.005
Ti	-0.101	0.090	-0.257	0.330
Fe	-0.478	-0.010	0.022	0.043
Mg	-0.524	-0.032	0.044	0.034
Ca	0.248	0.405	-0.252	-0.172
Na	0.238	0.030	0.057	0.211
K	0.085	0.105	0.570	0.372
P	-0.113	0.452	-0.124	-0.192
S	-0.132	0.249	-0.304	-0.205
Cl	-0.063	0.165	0.637	-0.388
Ni	-0.045	0.119	-0.074	0.646
Eigenval.	2.40	1.07	1.01	1.01
Cum.%	20.0	28.9	37.4	45.7

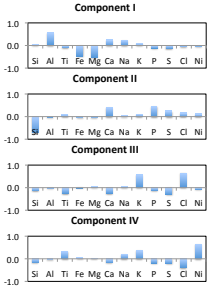

Preliminary conclusions

These PCA results cannot be uniquely interpreted, but they support the presence of excess plagioclase and a mobile (soluble) addition to the pre-impact material.

In both experiments, the first components have positive eigenvectors for Al and Ca and negative eigenvectors for Fe and Mg. **This suggests that the majority of the variance is controlled by an exchange of plagioclase composition for a mafic composition. Because it is found in the pure melt and in the partially crystallized portion, this component may represent excess plagioclase in the pre-impact material, supporting Rao et al. [1].**

In both experiments, the second components have negative eigenvectors for Si and positive for Ca, P, S, and Cl. **This component corresponds to the zonation in the melt visible in Figure 2. The PCA suggests there is an accompanying S and possibly Cl enrichment not apparent by visible inspection.**

Component IV in experiment 1 and Component III in experiment 2 have strong positive eigenvectors for K and Cl and variably negative eigenvectors for Ti and Ni. The association of K with Cl is apparent from WDS maps (Figure 1) but not from EDS maps (Figure 2). Ni, K, and Cl are all enriched in Martian soil [5-7], but while K and Cl are soluble and mobile, Ni is residual from weathered olivine. **This suggests a separate input into the pre-impact material for mobile elements than for elements from *in situ* weathering. This indicates a likely soil component in the precursor to Lithology C as suggested by Rao et al. [1].**

[1] Rao, M.N. et al. (1999) *GRL*, *26*, 3265-3268. [2] Rao, M.N., and McKay, D.S. (2002) *65th Annual Meeting of the Met. Soc.*, Abstract # 5042. [3] Newsom, H.E. and Haggerty (1999) *JGR*, *104*, 8717-8728. [4] Sutton, S.R. et al. (2002) *LPSC XXXIII*, Abstract #1278. [5] Gellert, R. et al. (2004) *Science 305*, 829-832. [6] Rieder, R., et al. (2004) *Science 306*, 1746-1749. [7] McSween, H.Y. et al. (2004) *Science 305*, 842-845.